JJCO Japanese Journal of Clinical Oncology

*Jpn J Clin Oncol 2010;40(1)85–89*
*doi:10.1093/jjco/hyp098*
Advance Access Publication 20 September 2009

Case Report

# A Case of Long-term Survival after Surgical Resection of Solitary Pulmonary Metastasis from Gastric Cancer

**Chiharu Tanai[1], Tetsuya Hamaguchi[1], Shun-ichi Watanabe[2], Hitoshi Katai[2], Naobumi Tochigi[3] and Yasuhiro Shimada[1]**

[1]Department of Medical Oncology, National Cancer Center Hospital, [2]Department of Surgical Oncology, National Cancer Center Hospital and [3]Pathology Division, National Cancer Center Research Institute, Tokyo, Japan

For reprints and all correspondence: Tetsuya Hamaguchi, Department of Medical Oncology, National Cancer Center Hospital, 5-1-1 Tsukiji, Chuo-ku, Tokyo 104-0045, Japan. E-mail: thamaguc@ncc.go.jp

Received April 13, 2009; accepted July 24, 2009

We describe a 60-year-old male patient who survived for a long period after pulmonary metastasectomy for gastric cancer. The patient initially underwent distal gastrectomy for gastric cancer. Seventeen months after the gastrectomy, surgical resection of solitary pulmonary metastasis was performed and following resection, the patient has survived without relapse for more than 5 years. Carefully selected patients have a good chance of benefiting from pulmonary metastasectomy for gastric cancer.

*Key words: solitary pulmonary metastasis – pulmonary metastasectomy – gastric cancer*

## INTRODUCTION

The majority of pulmonary metastasis after curative resection for gastric cancer present as carcinomatous lymphangitis or carcinomatous pleuritis, with few cases considered operable.

We describe here a case of long-term survival after surgical resection of solitary pulmonary metastasis from gastric cancer.

## CASE REPORT

A 60-year-old male was diagnosed with clinical stage IIIB gastric cancer (cT3N2M0). His medical history indicated appendicitis at 20 years of age and diabetes mellitus at 60 years. His father also had gastric cancer. From the time of diagnosis of gastric cancer, he stopped smoking after a 90-pack-year smoking history. He underwent distal gastrectomy with D2 lymphadenectomy and Roux-en-Y anastomosis at our institution. Gross examination of the resected specimen revealed a type 2 tumor (58 × 51 mm) arising from the greater curvature of the middle to the lower body of the stomach (Fig. 1). Microscopic examination revealed a well-differentiated adenocarcinoma with lymphatic but no venous invasion. The tumor had invaded the serosa but not the serosal surface. The proximal, distal and radial margins of the stomach were tumor-free. Regional lymph node metastases were found in 7 of 44 dissected lymph nodes (N1), arriving at a diagnosis of stage IIIA gastric cancer (pT3N1M0). The levels of the carcinoembryonic antigen (CEA) and carbohydrate antigen (CA) 19-9 were elevated to 13.3 ng/ml and 1504 U/ml, respectively, before surgery and returned to the normal level after surgery. Post-operative adjuvant chemotherapy was not administered (Fig. 1).

Computed tomography (CT) of the thoracic area on a follow-up visit 12 months after surgery revealed a 17 mm nodule in the left upper pulmonary lobe ($S_{1+2}$) with a regular margin, located adjacent to the pleura, and without any significant hilar or mediastinal lymphadenopathy. The CEA level was 5.0 ng/ml, which was within the normal range, but the CA19-9 level was elevated to 391 U/ml. Follow-up examinations showed that this pulmonary nodule gradually increased in size with accompanying elevation of the CEA and CA19-9 levels every month.

Three months after the first detection of the pulmonary nodule, the patient underwent transbronchial lung biopsy but the procedure failed to yield a definite diagnosis. At this point, it was difficult to distinguish gastric cancer pulmonary metastasis from primary lung cancer based on imaging.

The patient had no evidence of extrapulmonary metastases and was advised to undergo thoracic surgery. He was admitted to our institution 1 month later for pulmonary resection.

On examination, the patient showed no symptoms of disease and his vital signs were normal. Clinical examination showed mild anemia with a hemoglobin level of 10.7 g/dl. His complete blood cell count, serum chemistry and pulmonary function test were normal. Chest X-ray revealed an oval 29 mm tumor nodule in the peripheral zone of the left upper lung field (Fig. 2). CT of the thoracic area identified a well-circumscribed 25 × 18 mm nodule in the left upper pulmonary lobe ($S_{1+2}$) widely adjacent to the pleura (Fig. 3). Non-specific pleural thickening was observed, but no hilar, mediastinal lymphadenopathic, or other changes were evident.

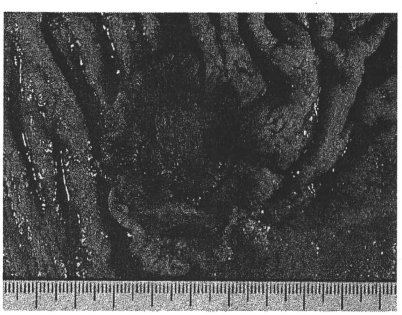

**Figure 1.** Gastrectomy specimen showing a 58 × 51 mm type 2 tumor in the greater curvature of the middle to the lower body of the stomach.

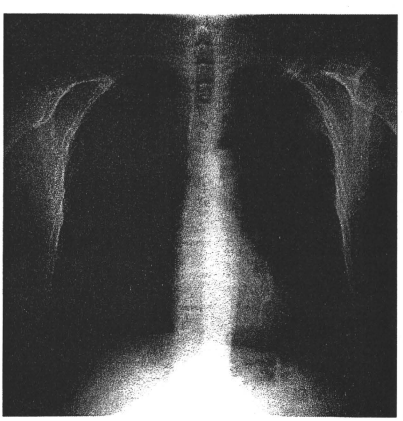

**Figure 2.** Chest X-ray image obtained 17 months after gastrectomy showing a nodule (29 mm) in the left upper lung field.

Thoracoscopy revealed adhesion between the left upper pulmonary lobe and the chest wall, but failed to identify the tumor. No pleural dissemination or effusion was detected. The patient underwent anterolateral thoracotomy through the 4th intercostal space. After dissecting the adhesion between the left upper pulmonary lobe and the chest wall, a hard tumor was identified. The tumor adhered strongly to the chest wall, suggesting possible chest wall invasion. Wedge resection of the tumor including the involved parietal pleura was performed. Intraoperative diagnosis was consistent with metastasis from gastric cancer.

Gross examination of the lesion demonstrated a 30 × 21 × 17 mm, elastic hard, yellowish white, smooth tumor with necrosis and scar (Fig. 4). Histopathological examination demonstrated morphological findings similar to those of the previously resected gastric cancer. The tumor was composed of tubular and partially papillary adenocarcinoma

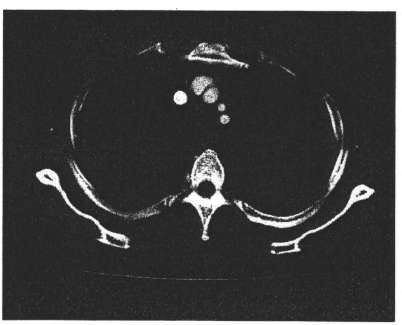

**Figure 3.** Chest CT performed 17 months after gastrectomy showing a nodule (25 × 18 mm) adjacent to thoracic wall in the left upper pulmonary lobe.

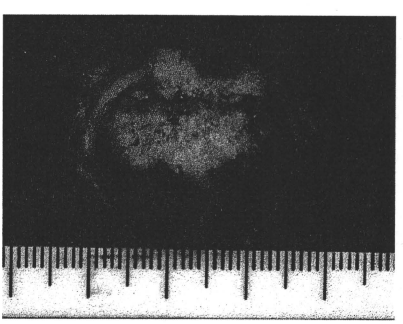

**Figure 4.** Wedge resected lung specimen showing a 30 × 21 × 17 mm elastic hard, yellowish white, smooth tumor.

with collagen fibers, compatible with gastric cancer metastases (Figs 5 and 6). Although the chest wall margin was tumor-free, the tumor had invaded the parietal pleura. Immunohistochemical staining showed negative for thyroid transcription factor-1 and Napsin A, suggesting the tumor was unlikely to be a primary lung adenocarcinoma. In light of the morphological similarity, we diagnosed the pulmonary tumor as a metastasis from gastric cancer.

On post-operative day 3, the patient developed surgical site infection and pyothorax, but recovered with surgical wound opening and thoracic drainage in 1 week. Four weeks later, the CEA and CA19-9 levels returned to the normal levels of 2.8 ng/ml and 32 U/ml, respectively. Follow-up examinations showed no evidence of recurrence 82 months after the initial gastrectomy and 65 months after the pulmonary resection.

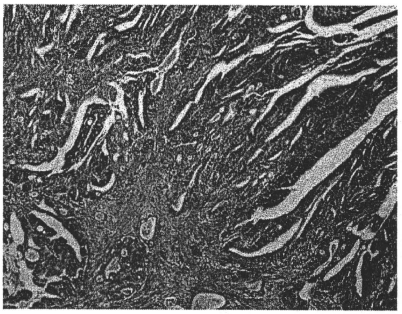

**Figure 5.** Resected stomach specimen containing a tubular structure (hematoxylin and cosin).

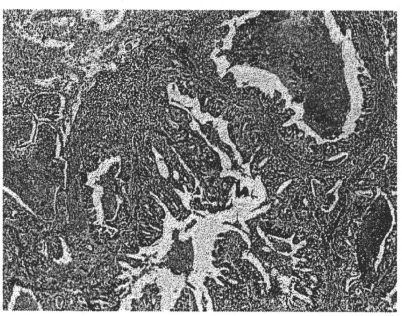

**Figure 6.** Resected lung specimen containing tubular and partially papillary adenocarcinoma, which resembles the stomach lesion (hematoxylin and cosin).

## DISCUSSION

Systematic circulation normally returns back to the lungs. Malignant tumors of organs supplied by the systematic circulation spread to the lungs intravascularly with high frequency. Pulmonary metastasis can thus be considered as a systematic disease in which tumor cells spread to the whole body, resulting in poor prognosis. However, long-term survival after surgical resection of pulmonary metastasis has been reported. According to the concept of the Cascade spreading process (1), some cases of pulmonary metastasis may be at the presystemic stage (i.e. tumor spread is still limited to the lungs which serve as an initial filter for trapping tumor cells) and can therefore benefit from surgical metastasectomy (2,3).

Pulmonary metastasectomy is considered when Thomford's criteria (4) are met as follows: (i) the patient must be a good risk for surgical intervention, (ii) the primary site is controlled, (iii) no other extrapulmonary metastases exist, or if present, it can be controlled by surgery or another treatment modality and (iv) pulmonary metastases are thought to be completely resectable. Importantly, the effectiveness of surgical resection differs largely by tumor characteristics, development pathway and sensitivity to chemotherapy and radiotherapy. Therefore, understanding the nature of each malignancy and proper selection of patients for surgery are required.

Pulmonary metastasectomy reportedly improves survival among patients with pulmonary metastasis from colorectal cancer, particularly those with a 5-year survival rate to higher than 35–50% and those with a 10-year survival rate by 20–30% (5–7). For patients who fulfill the indication criteria, surgical procedure should be considered. On the other hand, metastasectomy in poor prognostic patients with pulmonary metastasis from esophageal cancer, gastric cancer, hepatocellular carcinoma, biliary tract cancer and pancreatic cancer is rarely indicated (2). The majority of pulmonary metastasis from gastric cancer present as carcinomatous lymphangitis or carcinomatous pleuritis. A solitary lesion is rare and usually occurs in multiple forms if present, together with liver metastasis or peritoneal dissemination. Few of such cases are indicated for surgical resection.

The incidence of pulmonary metastasis from gastric cancer based on autopsy cases has been reported to be 22.4–52.3% (8–10). Surgically resectable solitary pulmonary metastasis accounts for a very low 0.1% in patients who have undergone curative resection for gastric cancer (11). Several reports have described pulmonary resection of metastasis from gastric cancer (11–18). Some reports showed that the primary site of solitary pulmonary metastasis tends to present more with a type 3 tumor than with a type 2 tumor, that the tumor appears from the upper site with esophageal invasion and that the tumor is a microscopically well- to moderately differentiated adenocarcinoma (15,19,20). All these reports showed tumor characteristics in a small number of cases and thus analysis of prognostic

**Table 1.** Characteristics of cases of primary gastric cancer

| Case | Age | Type of gastrectomy | Depth of invasion | Pathological stage | Disease-free interval (months) | Outcome after pulmonary resection |
|---|---|---|---|---|---|---|
| 1[a] | 61 | Distal | sc (T3) | IIIA | 17 | Alive at 65 months |
| 2 | 64 | Total | sc (T3) | III | 120 | Died at 35 months |
| 3 | 73 | Total | Unknown | Unknown | 37 | Died at 123 months |
| 4 | 61 | Total | ss (T2) | II | 59 | Died at 13 months |
| 5 | 50 | Distal | ss (T2) | IB | 46 | Died at 27months |
| 6 | 50 | Distal | ss (T2) | II | 20 | Died at 5 months |

[a]Present case.

factors is not possible. Pulmonary metastasectomy remains controversial considering the small number of cases that had fulfilled the surgical indication criteria but failed to show survival improvement by resection of solitary pulmonary metastasis (2,11,12). However, several cases with long-term survival after surgical resection of pulmonary metastasis from gastric cancer similar to the present case have been reported, indicating that appropriately selected patients may benefit from surgical resection (14–18).

Six cases including the present case presenting with solitary pulmonary metastasis from gastric cancer underwent pulmonary metastasectomy between 1997 and 2006 at our institution (Table 1). The median interval time between gastrectomy and the first detection of pulmonary metastasis was 29.5 months (13–115 months). Two cases whose lesion was difficult to distinguish from primary lung cancer underwent lobectomy, and the remaining four underwent partial resection. Two cases who received S-1 monotherapy as adjuvant chemotherapy after pulmonary resection relapsed with liver and pulmonary metastases, but the other four showed no evidence of relapse. The median follow-up time after the resection of pulmonary metastasis was 31 months (5–123 months). The 5-year survival rate after the resection of pulmonary metastasis was 33.3%. The median survival time for unresectable or recurrent gastric cancer was 7–10 months. Cases with solitary pulmonary lesions who will tolerate pulmonary resection and have prospects of a good postoperative quality of life and whose pulmonary lesions are thought to be completely resectable without any evidence of extrapulmonary metastasis have a good chance of improved survival, similar to the present case, and thus surgical procedure should be considered.

## CONCLUSION

We described a case of long-term survival after surgical resection of solitary pulmonary metastasis from gastric cancer. Although few cases can fulfill the indication criteria for pulmonary metastasectomy, selected patients have a good chance of benefiting from surgical resection. When a solitary pulmonary lesion is detected after surgical resection of gastric cancer, the same procedure should also be considered for the histologic differentiation of the metastasis from primary lung cancer.

## Conflict of interest statement

None declared.

## References


1. Viadana E, Bross IDJ, Pickren JW. The spread of blood-borne metastases in malignant lymphomas of man. *Oncology* 1976;33:123–31.
2. Kondo H, Nakayama H, Asamura H, Tsuchiya R, Naruke T. Surgical treatment for metastatic lung tumors. *J Jpn Surg Soc* 1998;99:299–302.
3. Kawano R, Yanada M, Kori T, Katsuragi N, Yokota T, Ikeda S, et al. Lung metastasectomy. *Kokyu* 2000;19:236–40 (in Japanese).
4. Thomford NR, Woolner LB, Clagett OT. The surgical treatment of metastatic tumors in the lungs. *J Thorac Cardiovasc Surg* 1965;49:357–63.
5. Davidson RS, Nwogu CE, Brentjens MJ, Anderson TM. The surgical management of pulmonary metastasis: current concepts. *Surg Oncol* 2001;10:35–42.
6. Pfannschmidt J, Dienemann H, Hoffman H. Surgical resection of pulmonary metastases from colorectal cancer: a systematic review of published series. *J Surg Oncol* 2007;84:324–38.
7. Saito H, Minamiya Y, Taguchi K, Nakagawa T, Ogawa J. Surgical treatment for pulmonary metastases from colorectal cancer. *Kyoubu Geka* 2003;56:35–40 (in Japanese).
8. Dupont JB, Lee GR, Burton GR, Cohn I. Adenocarcinoma of the stomach: review of 1,497 cases. *Cancer* 1978;41:941–7.
9. Ishii T, Ikegami N, Hosoda Y, Koide O, Kaneko M. The biological behavior of gastric cancer. *J Pathol* 1981;134:97–115.
10. Mori W, Adachi Y, Okabe H, Oota K. An analysis of 755 autopsied cases of malignant tumors—A statistical study of their metastasis. *Jpn J Cancer Clin* 1963;9:351–74.
11. Kanemitsu Y, Kondo H, Katai H, Nakayama H, Asamura H, Tsuchiya R, et al. Surgical resection of pulmonary metastases from gastric cancer. *J Surg Oncol* 1998;69:147–50.
12. Tamura M, Hiroshima K, Sugita K, Kobayashi S, Miyoshi S. Four cases of resected pulmonary tumor metastatic from gastric cancer. *Jpn J Lung Cancer* 2002;42:611–3.
13. Sawada T, Koike K, Sato M, Takahashi S. Two cases of resected metastatic lung tumor from gastric cancer. *J Jpn Assoc Chest Surg* 2006;20:686–93.
14. Sakaguchi K, Yamamoto M, Horio H. Resection of solitary pulmonary metastasis from gastric cancer. *Jpn J Lung Cancer* 2007;47:323–6.

15. Umehara Y, Miyahara T, Yoshida M, Oba N, Gotou H, Harada Y. Lung metastasis of stomach cancer—clinical and pathological assessment. *Jpn J Gastroenterol Surg* 1989;22:2772–7.
16. Umehara Y, Miyahara T, Yoshida M, Oba N, Harada Y. 2 cases of surgically resected pulmonary metastases from gastric cancer. *J Jpn Surg Soc* 1989;50:2578–82.
17. Tsumatori G, Ozeki Y, Aoki T, Watanabe M, Tanaka S, Aida S, et al. Five cases of surgically resected pulmonary metastases from gastric cancer: relation between the expression of carbohydrate antigens and metastasis. *J Jpn Assoc Chest Surg* 1998;12:85–91.
18. Nakayama H, Ichinose S, Kato Y, Ito H, Masui K, Kameda Y. Long-term survival after a surgical resection of pulmonary metastases from gastric cancer: report of a case. *Surg Today* 2008;38:150–3.
19. Yamauchi M, Yamada E, Miyaishi S, Nakazato H, Kato O, Kito T, et al. Pulmonary metastases from gastric cancer. *Jpn J Cancer Clin* 1982;28:1243–8.
20. Takafuji K, Takeda J, Aoyagi K, Yano S, Murakami N, Miyagi M, et al. Nodular pulmonary metastases from gastric cancer. *Jpn J Clin and Exp Med* 2002;79:76–8.

Brain Tumor Pathol (2011) 28:43–51
DOI 10.1007/s10014-010-0002-4

ORIGINAL ARTICLE

# Precise comparison of protoporphyrin IX fluorescence spectra with pathological results for brain tumor tissue identification

**Takehiro Ando · Etsuko Kobayashi · Hongen Liao · Takashi Maruyama · Yoshihiro Muragaki · Hiroshi Iseki · Osami Kubo · Ichiro Sakuma**

Received: 3 March 2010 / Accepted: 13 July 2010 / Published online: 25 December 2010


**Abstract** Photodynamic diagnosis is used during glioma surgery. Although some studies have shown that the spectrum of fluorescence was efficient for precise tumor diagnosis, previous methods to characterize the spectrum have been problematic, which can lead to misdiagnosis. In this paper, we introduce a comparison technique to characterize spectrum from pathology and results of preliminary measurement using human brain tissues. We developed a spectrum scanning system that enables spectra measurement of raw tissues. Because tissue preparations retain the shape of the device holder, spectra can be compared precisely with pathological examination. As a preliminary analysis, we measured 13 sample tissues from five patients with brain tumors. The technique enabled us to measure spectra and compare them with pathological results. Some tissues exhibited a good relationship between spectra and pathological results. Although there were some false positive and false negative cases, false positive tissue had different spectra in which intensity of short-wavelength side was also high. The proposed technique provides an accurate comparison of quantitative fluorescence spectra with pathological results. We found that spectrum analysis may reduce false positive errors. These results will increase the accuracy of tumor tissue identification.

**Keywords** 5-Aminolevulinic acid · Protoporphyrin IX · Fluorescence spectra · Photodynamic diagnosis

T. Ando (✉) · E. Kobayashi · H. Liao · I. Sakuma
Department of Bioengineering, Graduate School of Engineering, The University of Tokyo, Engineering building No.14, Room 722, Hongo 7-3-1, Bunkyo, Tokyo 113-8656, Japan
e-mail: take_and_o@bmpe.t.u-tokyo.ac.jp

T. Maruyama · H. Iseki · O. Kubo
Department of Neurosurgery, Neurological Institute, Tokyo Women's Medical University, Shinjuku, Tokyo 162-8666, Japan

Y. Muragaki · H. Iseki
Institute of Advanced Biomedical Engineering and Science, Tokyo Women's Medical University, Shinjuku, Tokyo 162-8666, Japan

## Introduction

Over recent decades, photodynamic diagnosis (PDD) has been studied for intraoperative tumor diagnosis, especially glioma. PDD uses autofluorescence or endogenous fluorescence materials [1–4], and the technique can be easily applied for clinical practice because the system is simple. In a number of clinical studies, 5-aminolevulinic acid (5-ALA)-induced protoporphyrin IX (PpIX) fluorescence has been used for intraoperative tumor diagnosis. Although 5-ALA and PpIX are natural substances produced by the human body, orally administrated 5-ALA accumulates in tumor cells and is converted to PpIX by heme biosynthesis. Accumulation of 5-ALA in a tumor cell may be caused by a damaged blood brain barrier (BBB) or iron (Fe)-metabolic enzyme defect, such as ferrochelatase [5]. However, the exact mechanism is still unknown.

Stummer et al. [1–3] introduced the use of the fluorescence surgical microscope to examine PpIX fluorescence for intraoperative tumor detection. They reported that some regions of brain and tumor tissue have different fluorescence characteristics (intensity and color) and assessed these tissues pathologically. Although this approach was appropriate for fluorescence-guided surgery, fluorescence measurement was not quantitative. A recent study of quantitative fluorescence measurement showed that PpIX spectrum shape is important to precisely detect tumor and

diagnose malignancy [6]. Another group reported that ultraviolet (UV) laser and white light reveal differences in the autofluorescence spectra between tumor and normal brain tissue [7, 8]. Although these quantitative studies found characteristic tumor tissue spectra when comparing them with pathological results, the comparison methods used have the following limitations. First, there is a possibility that a spectrum measurement point is different from a pathology examination point. This means that a spectrum characterization may not be correct. Second, because the spectrum measurement was performed after staining or fixation with formalin, the measured spectrum may be different from that of the raw tissue. To use the result in situ, raw tissue spectrum measurement is necessary. Finally, although tumor margin characterization is necessary for precise resection, these methods cannot determine spatial changes in spectra.

To solve these problems, we developed a spectrum scanning system that enables acquisition of raw tissue spectra distribution. Furthermore, our novel protocol makes it possible to precisely compare spectra with pathological results. In this paper, we introduce the technique we devised and present results of preliminary measurements.

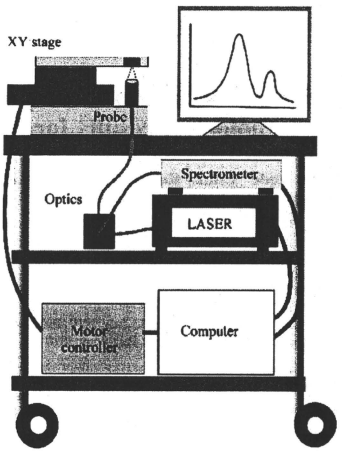


**Fig. 1** Overall view of the measurement system

## Materials and methods

### Measurement system

A spectrum-scanning system for 5-ALA-induced PpIX fluorescence was especially designed for both fluorescence measurement and fluorescence spectra comparison with pathological results. The system consists of an excitation laser (VLS405-SA3, Digital Stream), a spectrometer (WTC-111E B&W, TEK Inc.), optics, and a computer (Fig. 1). The excitation laser emits 405 nm of UV light, and the maximal output power is 15 mW. The spectrometer wavelength range is 300–850 nm. The measurement probe uses a coaxial optical system. All light paths are connected with optical fibers (core diameter 365 μm, multimode), and a dichroic mirror is used to separate excitation light and fluorescence. To insert a dichroic mirror in the light path, three collimator lenses are mounted to a cubic box. Angles and positions of all collimator lenses and the dichroic mirror angle can be adjusted to improve the coupling efficiency of the light. It is also equipped with a long-pass filter to separate strong reflected excitation light from the fluorescence signal. There are two achromatic lenses at the tip of the probe. The focal length of the fiber side lens is 19 mm, the object side is 30 mm, the working distance is 21.7 mm, and the lens diameter is 12.5 mm. The measurement spot diameter is evaluated using a phantom, the optical character of which is designed to match that of brain tissue. As a result, the system's measuring diameter is estimated as 0.8 mm.

To measure fluorescence spectra spatial changes, the measurement probe is fixed under an *XY* stage (SGSP20-35XY, Sigma Koki), and the sample tissues are then moved. A removable tissue holder that has a square 5-mm hole is set on the stage. One corner of the holder hole is cut down to make a shape mark. Because the holder location is registered to the *XY* stage coordinates, it is possible to follow the measuring position. In this study, spectra of 58 points were acquired from each sample tissue.

### Measurement protocol

To accurately compare spectra with pathological results, we devised the following measurement protocol:

1. Resected tissue was gently put in the measurement system tissue holder.
2. The spectrum of each point was measured by the system, and data were processed automatically.
3. After measurement, the tissue and the holder were put in liquid nitrogen to freeze the tissue.
4. The frozen tissue was taken out of the holder and sectioned using conventional methods.
5. The sectioned tissue was stained with hematoxylin–eosin (H&E).

Sectioning and staining were performed by a pathologist. Spectrometer exposure time and the laser power were

arbitrarily adjusted depending on each patient. Although this protocol is relatively complicated, because the frozen tissue retains the original shape of the holder and the measured surface can be maintained, it is possible to make a "holder-shaped" histological preparation. This preparation makes it possible to compare cell characteristics with the corresponding measurement points from the tissue shape and the *XY*-stage coordinates. Furthermore, because the spectrum is measured before freezing or staining, this method allows the use of raw brain tissue spectra for comparison. This means that the results can be directly applied to intraoperative measurement and resection.

### Data processing

Because measured spectra contain some noise, data were smoothed using the Savitzky–Golay method (25-point smoothing) [9]. After smoothing, spectra data were processed to extract each PpIX peak intensity and wavelength from raw data, which contain autofluorescence spectra. The procedure is as follows: First, we empirically approximated a curve of a background autofluorescence spectrum as a quartic function using the least mean squares (LMS) method. To draw the LMS curve, data sets of 590–610 and 747–913 nm were used (Fig. 2). After LMS curve (background) subtraction from raw data, PpIX peak intensity and wavelength were calculated as maximal intensity and its wavelength. We recorded not only the PpIX intensity but also intensity at 585 nm, which represents the intensity of short-wavelength side. These data were plotted on a contour map.

### Ex vivo measurement and pathological examination

Using the system we developed, we measured brain tissues resected during brain tumor operations at Tokyo Women's Medical University Hospital. At 7:30 a.m. on the day of the operation, 5-ALA at a dosage of 20 mg/kg body weight was orally administered to patients who were suspected of having a glioma. We targeted primary gliomas in five patients whose magnetic resonance image MRI results suggested that the tumors were grade III or IV. Measurement was performed at about 2:00 p.m. on the same day. Preparations for pathological examinations were made using the method mentioned earlier. Spectrometer exposure time was arbitrary set to 70–500 ms for each measurement point. Measurement time, including processing time, was approximately 10–40 s for each sample tissue. The pathological examinations were performed by a pathologist, and examiners were blinded to fluorescence measurement. All experimental protocols were approved by the Ethical Committee of Tokyo Women's Medical University.

## Results

Tumor types of each patient in this study were as follows:

Case 1: Glioblastoma multiforme (GBM)
Case 2: Anaplastic oligodendro-astrocytoma (AOA)
Case 3: Anaplastic oligodendroglioma (AO)
Case 4: Oligodendroglioma (O)
Case 5: GBM

We obtained one tissue from case 1, four from case 2, three from case 3, one from case 4, and four from case 5. Each tissue is represented by a number (case number) and alphabetic letters. Figures 3–5 show examples of the results of tissue0 2D, 5A, and 5D, respectively. In 2D (Fig. 3a), a tumor margin is visible from which the tumor spread gradually from the upper to the lower side; intensity distribution of PpIX corresponded to its tumor distribution (Fig. 3b). Interestingly, intensity at 585 nm was in the

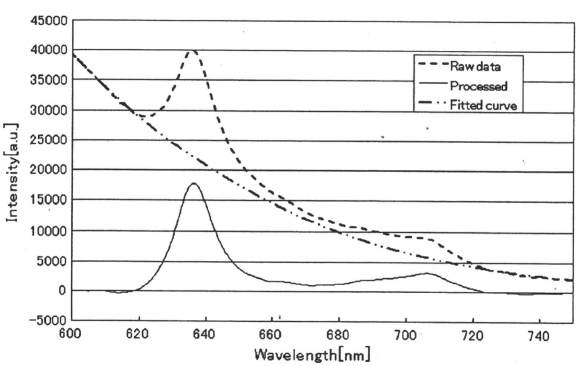


**Fig. 2** Background subtraction. *Fitted curve* baseline plotted by the approximate curve of a quartic function. *Raw data* raw spectrum acquired from a specimen. *Processed* processed spectrum plotted by subtracting the base curve from the raw spectrum

opposite distribution (Fig. 3c), which means that the intensity was higher in the normal area (585 nm was determined from the property of a long-pass filter and represents intensity of the short-wavelength side). The peak wavelength seemed almost the same throughout the region (Fig. 3d).

Although tissue 5A had no tumorous cells and seemed to be the region close to the cortex, the tissue had evidence of angiogenesis and gliosis, which can be identified by increased reactive astrocytes (Fig. 4a). Although the tissue was not a tumor, PpIX intensity was as high as that of tumor fluorescence throughout the entire region (Fig. 4b). Therefore, this was a false positive case of fluorescence measurement. However, the 585 nm intensity (Fig. 4c) was higher than that found in other tumor tissues from the same patient. The peak wavelength seemed the same throughout the region (the center region in Fig. 4d shows the error data caused by spectrometer saturation. Because the PpIX spectrum was saturated, the peak wavelength could not be calculated). Tissue 5D was from a tumor margin that had local accumulation of tumor cells (Fig. 5a). PpIX intensity distribution was well correlated with pathological results (Fig. 5b). The intensity of 585 nm had the opposite distribution to PpIX fluorescence (Fig. 5c). Furthermore, the peak wavelength also had a similar distribution (it shifted to the short side at the nontumor region) (Fig. 5d).

Tissue 1 was a tumor margin; the left side was tumor area and the right side the cortex. There was a blood vessel visible at the bottom left corner of the image that emitted strong PpIX fluorescence. However, the intensity at 585 nm was low in the vessel area but high around the vessel. Tissues 2A and 2C showed tumors all over the region, and PpIX intensity was high. Although pathological results showed that tissue 2A was homogeneously tumorous, varied PpIX intensity was observed. Tissue 2C had many vessels on the upper side, and PpIX intensity was relatively high in the region. Tissue 2B was tumorous over the entire tissue area, but only a small portion emitted PpIX fluorescence. Tissue 3A had a tumorous area, but PpIX intensity distribution did not exactly correspond to its tumor area. However, the intensity distribution of 585 nm, which has an opposite distribution to PpIX, was similar to pathological results. Although tissue 3B was not a tumor with blood vessels, PpIX spectrum or any other characteristic spectra were not acquired. Tissue 3C was not tumorous, and PpIX fluorescence was not acquired. Although tissue 4 was tumorous, with tumor cells distributed throughout the entire area, PpIX fluorescence could not be detected over the entire region. Tissue 5B had a nonuniform tumor distribution, including cell characteristics implicating necrosis. This sample might be close to the center of the tumor. PpIX intensity was also nonuniform but showed low intensity around the necrotic area. Tissue 5C was tumor tissue that had diffused astrocytoma cells. PpIX intensity was high over the entire region.

## Discussion

In this study, we introduced a novel technique to compare fluorescence spectra distribution of raw tissues with pathological results. We could confirm the necessity of a precise comparison because pathological results showed that cell characteristics varied with location, even when cell size was 5 × 5 mm, as in tissues 2D and 5D. Although we measured only 13 samples in this study, our comparisons showed some trends between spectra and pathological results, which can be divided into three groups. The first group had good correlation between spectra and pathological results, such as in tissues 2D and 5D. Furthermore, three tissues exhibited a relationship between pathological results and intensity distributions at 585 nm and PpIX peak wavelength. As noted earlier, intensity at 585 nm, which represents intensity of the short-wavelength side, has the opposite distribution to PpIX fluorescence. This light may come from an autofluorescence substance such as nicotinamide adenine dinucleotide (NADH), flavin, or lipofuscin [10]. In this study, considering excitation laser wavelength and emission spectrum, lipofuscin and flavin are anticipated to be the autofluorescence substances [11, 12]. Lipofuscin, in particular, appears in neuronal cells of aged patients and exhibits strong fluorescence, with a peak wavelength of approximately 560 nm. These results showed that the precise comparison of spectra with pathological results may increase diagnostic accuracy.

Some specimens, such as tissues 1 and 2C, exhibited high PpIX intensity around blood vessels. Because PpIX accumulates at tumor cells because of BBB disruption, PpIX is thought not to accumulate inside blood vessels. Although the high intensity of PpIX fluorescence was acquired at the blood vessel in tissue 1, the result was thought to be caused by infiltrating tumor around the blood vessel. Unfortunately, in this case, H&E preparation could not reveal the existence of infiltrating tumor cells because the measured point was very local, and preparation fixation was not optimum. In the case of tissue 2C, PpIX fluorescence intensity was relatively high around blood vessels. This result may demonstrate increased 5-ALA intake around blood vessels in which BBB are disrupted, which leads to considerable PpIX accumulation. Although we cannot show conclusive cause, tissue that has blood vessels should be investigated carefully.

The second group comprised false negative cases or cases in which fluorescence distribution was not correlated with pathological findings, such as tissues 2B and 4. There

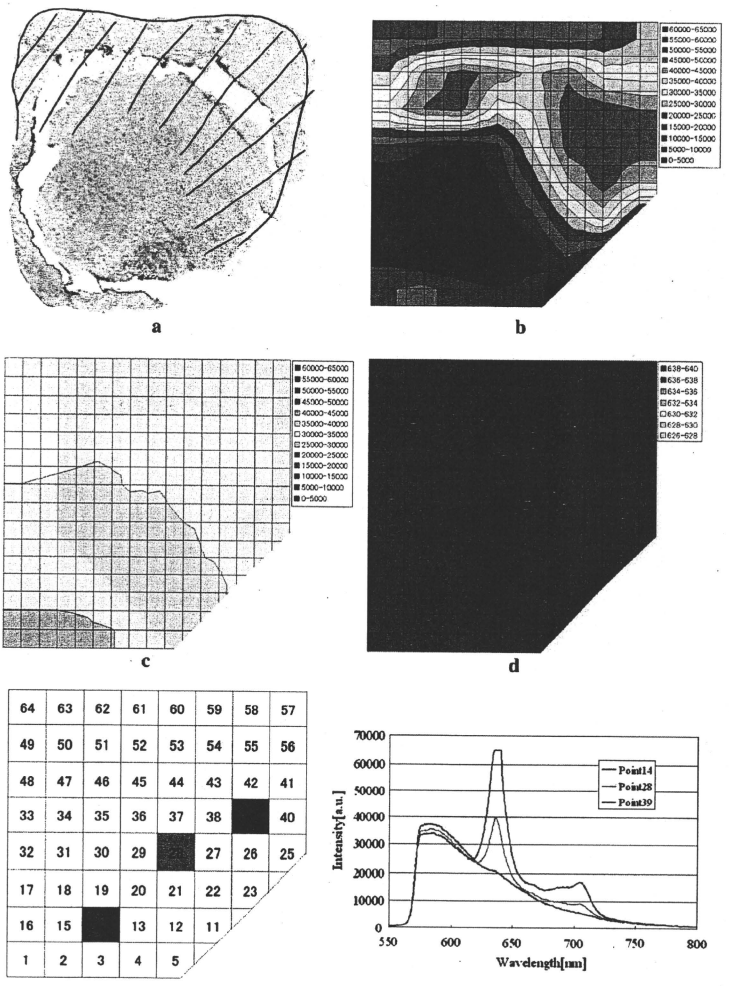


**Fig. 3** Results for tissue 2D. **a** Pathological result: this tissue seemed to be the tumor margin. **b** Intensity distribution of protoporphyrin IX (PpIX) fluorescence. **c** Intensity distribution at 585 nm. **d** Peak wavelength distribution of PpIX fluorescence. **e** Examples of measured points. **f** Example of measured spectra corresponding to measured points (**e**)

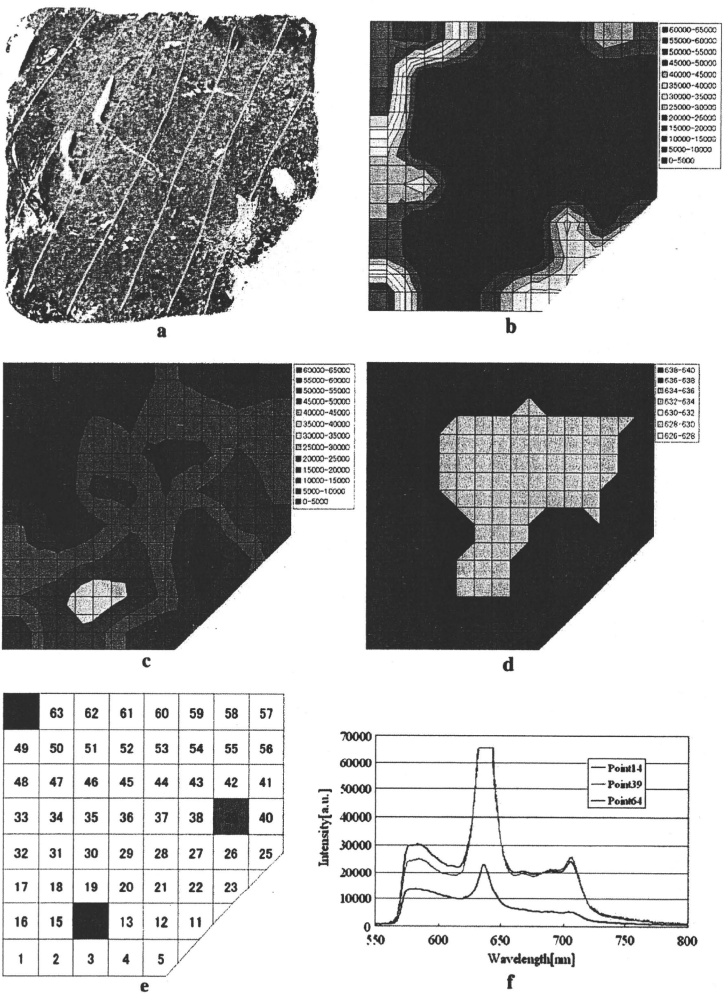


**Fig. 4** Results for tissue 5A. **a** Pathological result: this tissue was not tumorous but included reactive astrocytes. **b** Intensity distribution of protoporphyrin IX (PpIX) fluorescence. **c** Intensity distribution at 585 nm. **d** Peak wavelength of distribution of PpIX fluorescence. **e** Examples of measured points. **f** Example of measured spectra corresponding to measured points (**e**)

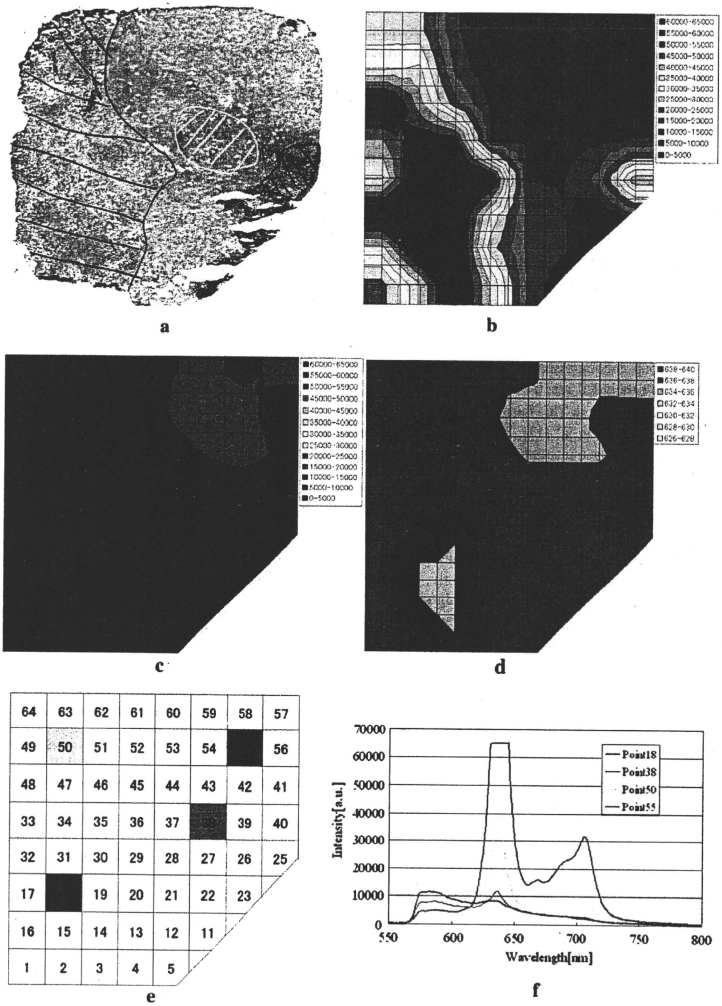


**Fig. 5** Results of tissue 5D. **a** Pathological result: this tissue had characteristic tumor distribution (*blue line*) and reactive astrocytes (*yellow line*). **b** Intensity distribution of protoporphyrin IX (PpIX) fluorescence. **c** Intensity distribution at 585 nm. **d** Peak wavelength distribution of PpIX fluorescence. **e** Examples of measured points. **f** Example of measured spectra corresponding to measured points (**e**)

are two possible causes. First, adherent blood on the tissue surface may prevent PpIX fluorescence measurement. Because red blood cells efficiently absorb UV light, which was used as the excitation laser, the light may not reach tissue PpIX [13–15]. In order to avoid damaging cells and changing there characteristics, we did not wash the tissue; however, as much excessive blood as possible had to be removed Second, not enough PpIX accumulated to emit fluorescence. The intake of 5-ALA may depend on the state of the BBB, and this influences the amount of PpIX. Because the BBB was not damaged severely in the low-grade tumor, PpIX may not emit fluorescence in such patients. Actually, tissue 4 was considered an oligodendroglioma, which is classified as grade II according to the World Health Organization classification [16]. Although we cannot control 5-ALA intake, our method can reveal limitations of 5-ALA-induced PpIX fluorescence.

The third group encompassed the false positive case of tissue 5A, which included reactive astrocytes that appear when brain tissue is injured. This false negative finding was also reported by Utsuki et al. [17]. The original astrocyte (not reactive), which is one of the glia cells, has many functions in the brain, such as maintaining brain structure, regulating ion concentration in the extracellular space, and supporting metabolic activity. The most important function of the astrocyte is that it controls the BBB [18, 19]. We hypothesized that the astrocytes changed their characteristics when they became reactive; subsequently, the BBB did not function efficiently, resulting in a higher 5-ALA intake. However, although PpIX fluorescence was detected as false positive, our measurement showed that the spectra of the tissue, including reactive astrocytes, were different from those of the tumor (short-wavelength intensity was high), which may reduce false positive error.

There are certain limitations to our technique. We deliberately changed the exposure time of the spectrometer because fluorescence intensity varied greatly with tissues and exceeded the dynamic range of the spectrometer. This problem prevents comparison among patients and results in an undesirable variety of data. However, the issue can be solved using exchangeable neutral-density filters and some estimation calculations. We developed a modified system that enables maintenance of the same measurement conditions for all patients, and now we measure tissues from various types of glioma using the modified system. Those data will show accurate tumor discrimination and the limitation of 5-ALA-induced PpIX fluorescence. Furthermore, we are working on a robotic system that uses 5-ALA-induced PpIX fluorescence for diagnosis and a midinfrared laser for tumor ablation [20]. The system allows intraoperative tumor identification and ultraprecise ablation. We expect that the method presented in this paper will provide a more accurate intraoperative diagnosis.

## Conclusion

We developed a spectrum scanning system that enabled precise comparison of tissue fluorescence spectra with pathological examination. Using the system, we measured 13 brain tissues from five patients and compared fluorescence spectra with pathology. Results showed that there was good correlation between fluorescence distribution and pathological results in high-grade tumor, and there were also false negative and false positive cases. We found that the spectrum of the false positive case, which had reactive astrocytes, was different from tumor spectrum. The results may reduce false positive error and lead to more accurate tumor discrimination PpIX fluorescence.

**Acknowledgment** This work was supported in part by grant for Translational Systems Biology and Medicine Initiative (TSBMI) and Grant-in-Aid for JSPS Fellows.

## References

1. Stummer W, Stepp H, Moller G et al (1998) Technical principles for protoporphyrin-IX-fluorescence guided microsurgical resection of malignant glioma tissue. Acta Neurochir (Wien) 140(10):995–1000
2. Stummer W, Novotny A, Stepp H et al (2000) Fluorescence-guided resection of glioblastoma multiforme by using 5-aminolevulinic acid-induced porphyrins: a prospective study in 52 consecutive patients. J Neurosurg 93(6):1003–1013
3. Stummer W, Pichlmeier U, Meinel T et al (2006) Fluorescence-guided surgery with 5-aminolevulinic acid for resection of malignant glioma: a randomised controlled multicentre phase III trial. Lancet Oncol 7(5):392–401
4. Chung YG, Schwartz JA, Gardner CM et al (1997) Diagnostic potential of laser-induced autofluorescence emission in brain tissue. J Korean Med Sci 12(2):135–142
5. Dailey HA, Smith A (1984) Differential interaction of porphyrins used in photoradiation therapy with ferrochelatase. Biochem J 223(2):441–445
6. Ishihara R, Katayama Y, Watanabe T et al (2007) Quantitative spectroscopic analysis of 5-aminolevuliniic acid-induced protoporphyrin IX fluorescence intensity in diffusely infiltrating astrocytomas. Neurol Med Chir (Tokyo) 47(2):53–57
7. Toms SA, Lin WC, Weil RJ et al (2005) Intraoperative optical spectroscopy identifies infiltrating glioma margins with high sensitivity. Neurosurgery 57(4 Suppl):382–391
8. Lin WC, Toms SA, Johnson M et al (2001) In vivo brain tumor demarcation using optical spectroscopy. Photochem Photobiol 73(4):396–402
9. Savitzky A (1964) Smoothing and differentiation of data by simplified least squares procedures. Anal Chem 36(8):1627–1639
10. Wagnieres G (1998) In vivo fluorescence spectroscopy and imaging for oncological applications. Photochem Photobiol 68:603–632
11. Yin D (1996) Biochemical basis of lipofuscin, ceroid, and age pigment-like fluorophores. Free Radic Biol Med 21(6):871–888
12. Eldred GE, Miller GV, Stark WS et al (1982) Lipofuscin: resolution of discrepant fluorescence data. Science 216(4547):757–759
13. Zijlstra WG, Buursma A, van der Roest WPM (1991) Absorption spectra of human fetal and adult oxyhemoglobin,

de-oxyhemoglobin, carboxyhemoglobin, and methemoglobin. Clin Chem 37(9):1633–1638
14. Faber DJ, Mik EG, Aalders MCG et al (2003) Light absorption of (oxy-)hemoglobin assessed by spectroscopic optical coherence tomography. Opt Lett 28(16):1436–1438
15. Faber DJ, Aalders MCG, Mik EG et al (2004) Oxygen saturation-dependent absorption and scattering of blood. Phys Rev Lett 93(2):028102
16. Louis DN, Ohgaki H, Wiestler OD et al (2007) The 2007 WHO classification of tumours of the central nervous system. Acta Neuropathol 114(2):97–109
17. Utsuki S, Oka H, Sato S et al (2007) Histological examination of false positive tissue resection using 5-aminolevulinic acid-induced fluorescence guidance. Neurol Med Chir (Tokyo) 47(5):210–213
18. Janzer RC, Raff MC (1987) Astrocytes induce bloodbrain barrier properties in endothelial cells. Nature 325(6101):253–257
19. Janzer RC (1993) The blood-brain barrier: cellular basis. J Inherit Metab Dis 16(4):639–647
20. Noguchi M, Aoki E, Yoshida D, Kobayashi E, Omori S, Muragaki Y, Iseki H, Nakamura K, Sakuma I (2006) A novel robotic laser ablation system for precision neurosurgery with intraoperative 5-ALA-induced PpIX fluorescence detection. MICCAI 4190:543–550

Langenbecks Arch Surg (2010) 395:545–549
DOI 10.1007/s00423-010-0642-1



ORIGINAL ARTICLE

# Improving prediction of lateral node spread in low rectal cancers—multivariate analysis of clinicopathological factors in 1,046 cases

**Kok-Yang Tan · Seiichiro Yamamoto · Shin Fujita · Takayuki Akasu · Yoshihiro Moriya**

Received: 25 January 2010 / Accepted: 22 March 2010 / Published online: 2 April 2010


**Abstract**
*Introduction* This study aims to search for independent predictors of lateral node metastasis in low rectal cancers.
*Materials and methods* We analyzed 1,046 patients who underwent curative resection for lower rectal cancer in our prospectively collected database. All lymph nodes were dissected from the fresh specimen, and their locations were documented prospectively according to the classification by the Japanese Society of Cancer of the Colon and Rectum.
*Results* More than 35% of the patients had demonstrated upward nodal metastasis in the direction of the inferior mesenteric vessels, while 11% demonstrated lateral node metastasis, which was present in 17.3% of patients with T3 and T4 lesions. Multivariate analysis revealed five factors to be statistically significant independent predictors of lateral node metastasis: female sex, tumors that were not well differentiated, pathological T3 and above, positive microscopic lymphatic invasion, and positive mesorectal nodes. Using the variables sex, differentiation, T stage, and mesorectal nodes as risk factors, because these could be elucidated preoperatively, the presence of lateral node metastasis was then analyzed according to the number of positive risk factors. When there were fewer than three positive factors, the risk of lateral nodal spread was low (4.5%). When three or more risk factors were positive, the odds of lateral node metastasis were more than 7.5 times higher ($p<0.001$).
*Conclusion* The findings of this study provide a scoring system that can be used to guide the clinician to the presence of lateral node metastasis in low rectal cancers.

**Keywords** Rectal cancer · Lateral node spread · Lymph nodes · Risk factors

## Introduction

Although the management of lateral node metastasis for low rectal cancers below the peritoneal reflection is still controversial [1–5], most authors agree on the importance of lateral lymph node metastasis in low rectal cancer [6], the reported incidence being between 13.8% [7] and 17.3% for pT3 and above lesions [8, 9].

It was previously elegantly demonstrated that it is the lower rectal cancers with deeper invasion that are associated with lateral node metastasis [9, 10]. However, independent risk factors of lateral node metastasis in low rectal cancers alone have yet to be elucidated. Some studies have attempted to identify some of these factors [8, 11], but these studies were relatively small and used a selected cohort. With the advent of better imaging modalities of the rectum and pelvis (transrectal ultrasonography, high-resolution computed to-

All listed authors contributed to the conception of the paper, data collection, and interpretation. All gave input during drafting and revision of the article and its final approval.

This paper is not funded by any source. There are no potential conflicts of interests of any of the authors with regards to the findings in this paper.

K.-Y. Tan · S. Yamamoto (✉) · S. Fujita · T. Akasu · Y. Moriya
Colorectal Surgery Division,
National Cancer Center Hospital, 5-1-1 Tsukiji,
Chuo-ku, Tokyo 104-0045, Japan
e-mail: seyamamo@ncc.go.jp

K.-Y. Tan
e-mail: kokyangtan@gmail.com

K.-Y. Tan
Department of Surgery, Alexandra Health,
Singapore, Singapore

mography (CT), and magnetic resonance imaging (MRI)), accurate preoperative evaluation of the presence of lateral node spread became possible; however, the quality of preoperative imaging differs among institutions, and there is a need to identify low rectal cancer patients at high risk of lateral spread even when imaging studies are negative.

This study aimed to identify independent predictors of lateral node metastasis in low rectal cancers by analyzing a large number of cases. This in turn will then help colorectal surgeons make treatment decisions for their patients preoperatively.

## Materials and methods

Patients who underwent curative resection for rectal cancer below the peritoneal reflection between January 1980 and October 2008 at the National Cancer Center, Tokyo were reviewed. The level of the tumor was documented at the time of the resection. Surgery for low rectal cancers was low anterior resection, abdomino-perineal resection, Hartmann's operation, or pelvic exenteration for locally advanced tumors. All patient data were obtained from a prospectively collected database in the department.

The practice of lateral node dissection has evolved over the years. Routine bilateral node dissection for all clinical stage I, II, and II lower rectal cancers in the 1980s and early 1990s. With the advent of better imaging modalities of the rectum and pelvis (transrectal ultrasonography, high-resolution CT, and MRI) in the latter half of the 1990s, a more selective approach to patient selection was undertaken. Lateral node dissection was undertaken for patients with a clinical diagnosis of site in the lower rectum (distal to the middle Houston valve) and depth of invasion that was staged clinically to be T3 and above. Lateral node dissection was also undertaken when preoperative pelvic imaging using high-resolution CT or pelvic MRI revealed a lymph node in the lateral region that was more than 1 cm in size or if the surgeon found a clinically suspicious lateral node intraoperatively. Although, with these selection criteria, some patients with lateral lymph node metastases may have been missed; however, most of the patients who did not undergo lateral node dissection were patients with moderate to high risk for radical surgery, with relatively early stage tumors. We believe that the inclusion of these patients have the increased risk of bias because there are no data regarding lateral node status; therefore, the patients without lateral node dissection were excluded from the present study.

Adjuvant postoperative radiotherapy for low rectal cancers is not performed routinely after lateral node dissection. Preoperative radiotherapy is administered in locally advanced cases (clinical T4) and tumors that are very low (<5 cm from the anal verge) with bilateral lateral node involvement as judged by preoperative imaging [12].

Patients enrolled in the JCOG 0212* (https://center.umin.ac.jp/cgi-open-bin/ctr/ctr.cgi?function=brows&action=brows&recptno=R000000068&type=summary&language=E) study were included in this present study. Patients that were randomized to TME alone in this trial were followed up carefully, and their pattern of recurrence was documented if any. Patients found to have local recurrence in the region of the lateral nodes were classified as having positive lateral nodes at the primary resection.

There were 1,200 resection cases, and patients with no data on lateral node status were excluded. After exclusion, 1,046 patients from our database were analyzed.

All definitions are according to those set by the Japanese Society of Cancer of the Colon and Rectum [13]. Parameters analyzed were patient sex, tumor morphological type, tumor size measured from a freshly pinned out specimen, tumor differentiation, pathological T stage, and microscopic lymphatic and venous invasion in sections of the tumor. All lymph nodes were dissected from the fresh specimen, and their locations according to the classification by the Japanese Society of Cancer of the Colon and Rectum were documented prospectively.

Bivariate analysis was performed using chi [2] test using SPSS for Windows (SPSS Inc., Chicago, USA), version 15.0. Results are expressed as odds ratios with 95% confidence intervals. Stepwise logistic regression analysis was used in multivariate analysis to identify parameters that independently affect outcome. Only factors that were found on bivariate analysis to be statistically significant ($p<0.05$) were used in multivariate analysis.

## Results

Patient and tumor characteristics are shown in Table 1. These characteristics are similar to other rectal cancer cohorts described in the literature. The median number of lymph nodes harvested was 30±19.8. Upward nodal metastasis in the direction of the inferior mesenteric vessels were present in 35.9% ($n$=377) of patients, while 11% ($n$=116) had demonstrated lateral node metastasis. Bivariate analysis revealed that female sex, size more than 3 cm, tumors that were not well differentiated, pathological T3 and above, positive microscopic lymphatic, and venous invasion in the tumor and positive mesorectal nodes were all statistically significant risk factors of lateral node metastasis (Table 1). Only 3.5% of patients with T1 and T2 lesions had lateral node metastasis, while the value was 17.3% for patients with T3 and T4 lesions.

Upon multivariate analysis of these factors, five factors were found to be statistically significant independent predictors of lateral node metastasis. These were female sex, tumors that were not well differentiated, pathological T3 and

**Table 1** Patient and tumor characteristics

| | Lateral lymph node status | | *p* Value |
|---|---|---|---|
| | Positive ($n$=113) | Negative ($n$=933) | |
| Sex ratio (male/female) | 60:53 | 646:287 | 0.001 |
| Mean age (year) | 58.60±10.99 | 59.48±11.28 | 0.433 |
| Pathological T stage[a] | | | |
| T1 ($n$=189) | 1 | 188 | <0.001 |
| T2 ($n$=301) | 16 | 285 | |
| T3 ($n$=516) | 81 | 435 | |
| T4 ($n$=32) | 14 | 18 | |
| Ratio of T1+T2/T3+T4 | 17:95 | 473:453 | <0.001 |
| Differentiation | | | |
| Well ($n$=525) | 27 | 498 | <0.001 |
| Moderately ($n$=463) | 66 | 397 | |
| Poorly ($n$=25) | 7 | 18 | |
| Mucinous or signet ring cell ($n$=33) | 13 | 20 | |
| Ratio of well differentiated/not well differentiated | 27:86 | 498:435 | <0.001 |
| Microscopic tumor lymphovascular invasion | | | |
| Lymphatic invasion (positive/negative) | 78:35 | 358:575 | <0.001 |
| Venous invasion (positive/negative) | 65:48 | 366:567 | <0.001 |
| Mean tumor size in cm (range) | | | |
| <3 cm:>3 cm | 3:102 | 151:660 | <0.001 |
| Mesorectal nodes status (positive/negative) | 84:29 | 293:640 | <0.001 |

[a] Data missing for eight patients

above, positive microscopic lymphatic invasion, and positive mesorectal nodes (Table 2). Of these five, microscopic lymphatic invasion cannot be elucidated preoperatively.

Using sex, differentiation, T stage and mesorectal nodes as risk factors, the presence of lateral node metastasis was then analyzed according to the number of positive risk factors (Table 3). When there were fewer than three positive factors, the risk of lateral nodal spread was low (4.7%). When three or more risk factors were positive, the odds of lateral node metastasis were more than 7.5 times higher (hazard ratio 7.567, 95% CI 4.941–11.587, $p$<0.001).

When subgroup analysis was performed for T1 and T2 lesions only, 17 of 490 patients (3.5%) had lateral node metastasis. This became 36.4% (8 of 22) when the remaining three risk factors were present (hazard ratio 29.143, 95% CI 9.791–86.745).

## Discussion

While the practice of lateral node dissection has been abandoned by most Western centers, in Japan, this procedure has remained part of the surgical treatment of rectal cancers with many important refinements since the 1970s [14, 15]. As such, it is not surprising that most of the data on lateral node metastasis in rectal cancers are from Japan [6]. Important data on the risk factors of lateral node metastasis were reported by Sugihara et al. [9] who performed multivariate analysis on 930 patients from 12 centers in Japan with upper and lower rectal cancers. The patients were treated between 1991 and 1998. After multivariate analysis of all pathological factors, only three were found to be independent risk factors: female sex, low rectal lesions, and tumors more than 4 cm in size; however, when only factors that can be

**Table 2** Multivariate analysis for independent risk factors for lateral nodal spread

| | Hazard ratio | 95% CI | *p* |
|---|---|---|---|
| Male sex | *0.441* | *0.280–0.696* | *<0.001* |
| Size 3 cm and above | 2.829 | 0.806–9.932 | 0.105 |
| Not well differentiated | *2.251* | *1.354–3.744* | *0.002* |
| pT3 and above | *2.775* | *1.425–5.404* | *0.003* |
| Positive lymphatic invasion | *1.935* | *1.176–3.183* | *0.009* |
| Positive vascular invasion | 1.298 | 0.822–2.051 | 0.263 |
| Mesorectal nodes positive | *3.101* | *1.829–5.256* | *<0.001* |

Significant factors in italics

Table 3 Risk of lateral node spread based on number of positive risk factors

| Number of factors positive | N | Lateral node spread | Percentage |
|---|---|---|---|
| 0 | 173 | 1 | 0.6 |
| 1 | 297 | 8 | 2.7 |
| 2 | 290 | 27 | 9.3 |
| 3 | 217 | 50 | 23.0 |
| 4 | 61 | 26 | 42.6 |

assessed preoperatively were analyzed, T stage of T3 and above and non-well differentiation became independent predictors as well. Of these factors, location in the lower rectum had the highest hazard ratio of 6.4 (95% CI 3.5–11.8). For this reason, we chose to only concentrate on tumors below the peritoneal reflection for this study.

For tumors of the lower rectum only, several studies have reported the risk factors for lateral spread. Ueno et al. [8] found low placement of the tumor, differentiation, and mesenteric nodes as independent risk factors in 237 patients, while in a smaller study on 96 patients, multivariate analysis was not performed likely due to inadequate numbers. The aim of this study was to analyze risk factors in a large number of patients so as to reduce random sampling error, thus giving the most accurate representation of patients with low rectal cancers. In order to obtain a large sample size, operations dating back to 1980 were included; as such, some factors including preoperative CT could not be included in this analysis. However, this study is very likely able to give the most accurate correlation of clinicopathological factors with lateral node spread to date.

In this study on a large number of patients, the most important risk factors found to have independently the highest hazard ratios are not dissimilar to those elucidated previously [8, 9]. In recent years, priority for lateral node dissection has been given to patients with low rectal lesions, T3 and above lesions, and when mesorectal nodes are detected, and this study confirms that this is a sound approach.

The findings from this study and the utility of a risk factor scoring system may further help surgeons to select patients for the management of lateral node metastasis. This may further be augmented by preoperative imaging modalities for lateral nodes. Female sex and cell differentiation can be easily determined preoperatively. A slightly bigger challenge is the clinical diagnosis of the T stage and the presence of mesorectal or lateral nodes using imaging modalities. Transrectal ultrasonography and pelvic MRI have been found to be very good modalities for determining the T stage and the presence of mesorectal nodes [16, 17]. An institution should choose the modality based on its own expertise and review their results, correlating preoperative diagnosis to pathological diagnosis. We feel that it will not be difficult for institutions to use this scoring system to predict the risk of lateral spread.

There has been much less experience on imaging involving lateral nodes, but increasing numbers of studies have emerged showing some efficacy using CT or MRI [18–20]. However, the problem of overstaging based on a single preoperative imaging modality is very real [6]. As such, single modality imaging can only be used as an adjuvant and not as sole assessment for the presence of positive lateral nodes. It is very likely that combined imaging and correlation with clinicopathological factors will provide the best accuracy. In another study by our center, focusing on patients with only advanced upper and lower rectal cancers with preoperative CT, it was demonstrated that similar risk factors used in combination with preoperative CT was most accurate in predicting lateral node spread [21].

One interesting finding from this study is that of patients with T1 or T2 lesions with lateral node metastasis. While the overall rate of lateral node metastasis was low, 3.5% of patients in this group had all three risk factors, and in this group of patients, more than one third had lateral node spread. We feel that for this small group of patients with three positive risk factors, imaging for lateral nodes should be performed with a view of managing the lateral nodes.

A recent study found that the approach to the management of cancers of the lower rectum by our center (described earlier) yielded a 5-year local recurrence rate of only 6.6% [22]. In an earlier study, we found that in patients with pathological N1 lymph node metastasis, the 5-year disease-free survival rate was 73.3% in patients who underwent lateral pelvic node dissection compared to 35.3% among those who did not [2]. These results suggest that it is important to address lateral node metastasis.

The treatment approach for patients with a high risk of lateral node metastasis is still very controversial and not within the scope of this discussion. It should be noted, however, that the survival rates of patients with lateral nodes do not suggest that it is a systemic disease [6, 9]. Most Western surgeons will employ radiotherapy, but there are now emerging reports of long-term adverse effects and functional problems from radiotherapy for rectal cancers [23–25]. On the other hand, the Japanese have been developing and refining lateral node dissection and have been achieving improved functional results over the recent years [15]. In Japan, the JCOG 0212 trial was started from June 2003. This is a multicenter trial randomizing patients to total mesorectal excision (TME) or TME plus lateral node dissection. The main aim of this trial was to answer the question of efficacy of lateral node dissection when there is no clinical imaging diagnosis of lateral node metastasis. The results of JCOG 0212 will only be available around 2016.

It cannot be denied that lateral node metastasis exists and should not just be passed off as systemic disease, and it is important to identify patients with a high-risk of lateral spread. These high-risk patients should be counseled carefully about these risks, implications, and treatment modalities. There are advantages and disadvantages to both radiotherapy and lateral node dissection, and it is important for patients to make a well-informed decision regarding the treatment of their cancer.

## Conclusion

The findings of this study provide a scoring system that can be used to guide the clinician to the presence of lateral node metastasis in low rectal cancers. When there were fewer than three positive factors, the risk of lateral nodal spread was low (4.7%). When three or more risk factors were positive, the odds of lateral node metastasis were more than 7.5 times higher. Considering the outcome of the present study together with the analysis of JCOG 0212 trial, we believe that selection for lateral lymph node dissection can be improved.

## References


1. Moriya Y, Hojo K, Sawada T, Koyama Y (1989) Significance of lateral node dissection for advanced rectal carcinoma at or below the peritoneal reflection. Dis Colon Rectum 32(4):307–315
2. Fujita S, Yamamoto S, Akasu T, Moriya Y (2003) Lateral pelvic lymph node dissection for advanced lower rectal cancer. Br J Surg 90(12):1580–1585
3. Kim TH, Jeong SY, Choi DH et al (2008) Lateral lymph node metastasis is a major cause of locoregional recurrence in rectal cancer treated with preoperative chemoradiotherapy and curative resection. Ann Surg Oncol 15(3):729–737
4. Mortenson MM, Khatri VP, Bennett JJ, Petrelli NJ (2007) Total mesorectal excision and pelvic node dissection for rectal cancer: an appraisal. Surg Oncol Clin N Am 16(1):177–197
5. Koch M, Kienle P, Antolovic D et al (2005) Is the lateral lymph node compartment relevant? Recent Results Cancer Res 165:40–45
6. Yano H, Moran BJ (2008) The incidence of lateral pelvic side-wall nodal involvement in low rectal cancer may be similar in Japan and the West. Br J Surg 95(1):33–49
7. Moriya Y, Sugihara K, Akasu T, Fujita S (1997) Importance of extended lymphadenectomy with lateral node dissection for advanced lower rectal cancer. World J Surg 21(7):728–732
8. Ueno M, Oya M, Azekura K et al (2005) Incidence and prognostic significance of lateral lymph node metastasis in patients with advanced low rectal cancer. Br J Surg 92(6):756–763
9. Sugihara K, Kobayashi H, Kato T et al (2006) Indication and benefit of pelvic sidewall dissection for rectal cancer. Dis Colon Rectum 49(11):1663–1672
10. Steup WH, Moriya Y, van de Velde CJ (2002) Patterns of lymphatic spread in rectal cancer. A topographical analysis on lymph node metastases. Eur J Cancer 38(7):911–918
11. Wu ZY, Wan J, Li JH et al (2007) Prognostic value of lateral lymph node metastasis for advanced low rectal cancer. World J Gastroenterol 13(45):6048–6052
12. Fujita S, Yamamoto S, Akasu T, Moriya Y (2008) Outcome of patients with clinical stage II or III rectal cancer treated without adjuvant radiotherapy. Int J Colorectal Dis 23(11):1073–1079
13. Japanese Research Society for Cancer of the Colon and Rectum (1983) General rules for clinical and pathological studies on cancer of the colon, rectum and anus. Part II. Histopathological classification. Jpn J Surg 13(6):574–598
14. Moriya Y, Sugihara K, Akasu T, Fujita S (1995) Nerve-sparing surgery with lateral node dissection for advanced lower rectal cancer. Eur J Cancer 31A(7–8):1229–1232
15. Moriya Y (2006) Function preservation in rectal cancer surgery. Int J Clin Oncol 11(5):339–343
16. Rovera F, Dionigi G, Boni L et al (2007) The role of EUS and MRI in rectal cancer staging. Surg Oncol 16(Suppl 1):S51–S52
17. Nicholls RJ, Tekkis PP (2008) Multidisciplinary treatment of cancer of the rectum: a European approach. Surg Oncol Clin N Am 17(3):533–551, viii
18. Matsuoka H, Nakamura A, Masaki T et al (2007) Optimal diagnostic criteria for lateral pelvic lymph node metastasis in rectal carcinoma. Anticancer Res 27(5B):3529–3533
19. Arii K, Takifuji K, Yokoyama S et al (2006) Preoperative evaluation of pelvic lateral lymph node of patients with lower rectal cancer: comparison study of MR imaging and CT in 53 patients. Langenbecks Arch Surg 391(5):449–454
20. Yano H, Saito Y, Takeshita E et al (2007) Prediction of lateral pelvic node involvement in low rectal cancer by conventional computed tomography. Br J Surg 94(8):1014–1019
21. Fujita S, Yamamoto S, Akasu T, Moriya Y (2009) Risk factors of lateral pelvic lymph node metastasis in advanced rectal cancer. Int J Colorectal Dis 24:1085–1090
22. Kusters M, van de Velde CJ, Beets-Tan RG et al (2009) Patterns of local recurrence in rectal cancer: a single-center experience. Ann Surg Oncol 16(2):289–296
23. Birgisson H, Pahlman L, Gunnarsson U, Glimelius B (2008) Late gastrointestinal disorders after rectal cancer surgery with and without preoperative radiation therapy. Br J Surg 95(2):206–213
24. Birgisson H, Pahlman L, Gunnarsson U, Glimelius B (2007) Late adverse effects of radiation therapy for rectal cancer—a systematic overview. Acta Oncol 46(4):504–516
25. Birgisson H, Pahlman L, Gunnarsson U, Glimelius B (2005) Adverse effects of preoperative radiation therapy for rectal cancer: long-term follow-up of the Swedish Rectal Cancer Trial. J Clin Oncol 23(34):8697–8705

Original article

# Origin of presacral local recurrence after rectal cancer treatment

M. Kusters[1], C. Wallner[2], M. M. Lange[3], M. C. DeRuiter[4], C. J. H. van de Velde[3], Y. Moriya[5] and H. J. T. Rutten[1]

[1]Department of Surgery, Catharina Hospital, Eindhoven, [2]Department of Anatomy, Embryology and Physiology, Amsterdam University Medical Centre, Amsterdam, and Departments of [3]Surgery and [4]Anatomy and Embryology, Leiden University Medical Centre, Leiden, The Netherlands, and [5]Department of Colorectal Surgery, National Cancer Center Hospital, Tokyo, Japan

*Correspondence to:* Dr M. Kusters, Department of Surgery, Catharina Hospital Eindhoven, Postbox 1350, 5602 ZA, Eindhoven, The Netherlands (e-mail: miranda.kusters@cze.nl)

**Background:** The objective of this study was to obtain detailed anatomical information about the lateral lymph nodes, in order to determine whether they might play a role in presacral local recurrence of rectal cancer after total mesorectal excision without lateral lymph node dissection.

**Methods:** Ten serially sectioned human fetal pelvises were studied at high magnification and a three-dimensional reconstruction of the fetal pelvis was made.

**Results:** Examination of the histological sections and the three-dimensional reconstruction showed that lateral lymph node tissue comprises a major proportion of the pelvic tissue volume. There were no lymph nodes located in the presacral area. Connections between the mesorectal and extramesorectal lymph node system were found in all fetal pelvises, located below the peritoneal reflection on the anterolateral side of the fetal rectum. At this site middle rectal vessels passed to and from the mesorectum, and branches of the autonomic nervous system bridge to innervate the rectal wall.

**Conclusion:** The findings of this study support the hypothesis that tumour recurrence might arise from lateral lymph nodes.

Paper accepted 18 May 2010

Published online 16 July 2010 in Wiley Online Library (www.bjs.co.uk). **DOI:** 10.1002/bjs.7180

## Introduction

Since the introduction of total mesorectal excision (TME) combined with neoadjuvant (chemo)radiation, locally recurrent rectal cancer has become less common. Local recurrence is associated with serious morbidity and shortened life expectancy[1]. The presacral subsite is the most prominent site of local recurrence in both early and advanced rectal cancer[2–5].

The genesis of presacral local recurrence is puzzling, as the presacral plane is the easiest plane of dissection during surgery and the presacral area is almost always included in the radiation volume. Several hypotheses can be made regarding the possible aetiology. The first is that positive margins lead to spillage of tumour cells, which accumulate in the presacral space by the force of gravity and develop into presacral local recurrence. In the TME trial, 75 per cent of presacral local recurrences occurred after abdominoperineal resection (APR) and 29 per cent of the APR specimens had positive margins[6]. In a study of locally advanced rectal carcinoma treated surgically in Catharina Hospital, Eindhoven, margin positivity was significantly associated with presacral local recurrence[5], making this theory plausible. However, even after exclusion of margin-positive operations in that study, presacral local recurrence was still common; tumour cells must have been left behind despite the negative margins.

Alternatively, tumour cells that are pumped into the lateral lymph flow routes during surgical manipulation might leak back into the surgical field postoperatively. This hypothesis is supported by the finding that Japanese patients had more local recurrences when the lateral lymph nodes on one side of the pelvis were left behind than when a bilateral lymph node dissection was performed[7]. This would explain why presacral local recurrence is more common in advanced disease than in limited disease, as lateral spread occurs mostly in high-stage tumours[8].